Environ Monit Assess (2016) 188:561
DOI 10.1007/s10661-016-5570-2

Sap flow characteristics and their response to environmental variables in a desert riparian forest along lower Heihe River Basin, Northwest China

Wei Li · TengFei Yu · XiaoYan Li · ChunYan Zhao

Received: 11 January 2016 / Accepted: 31 August 2016

Abstract Hysteresis, related to tree sap flow and associated environmental variables, plays a critical ecological role in the comprehensive understanding of forest water use dynamics. Nevertheless, only limited researches related to this unique ecological phenomenon have been conducted to date in desert riparian forests under extreme arid regions. *Populus euphratica Oliv* sap flow velocity (V_S) was measured during the 2012 growing season using the heat ratio method, at the same time as environmental variables, such as photosynthetically active radiation (PAR), vapor pressure deficit (VPD), and leaf water potential. We found clockwise patterns of hysteresis between V_S and VPD but anticlockwise patterns between V_S and PAR. Pronounced hysteretic V_S lag time, a function of PAR and VPD, was approximately 1.0~1.5 and −0.5 h, respectively. Hysteresis was primarily caused by the biophysical declining in canopy conductance. Sigmoid response of V_S to synthetic meteorological variables was enhanced by approximately 56 % after hysteresis calibration to sunny days. Consequently, hysteresis can be seen as a protection mechanism for plants to avoid the overlapping of peak V_S and environmental variables. Furthermore, the consistent presence of hysteresis suggested that estimating of plant water use in large temporal and spatial models may require certain provisions to different V_S responses to variables between morning and afternoon and between seasons.

Keywords Sap flow · Hysteresis · Principal component analysis · Canopy conductance · *Populus euphratica*

W. Li · X. Li
College of Resources Science and Technology, Beijing Normal University, Beijing 100875, China

W. Li
e-mail: liwei19870316@hotmail.com

W. Li · X. Li (✉)
State Key Laboratory of Earth Surface Processes and Resource Ecology, Beijing Normal University, Beijing 100875, China
e-mail: xyli@bnu.edu.cn

T. Yu · C. Zhao
Northwest Institute of Eco-Environment and Resources, Chinese Academy of Sciences, Lanzhou 730000, China

T. Yu
e-mail: yutf@lzb.ac.cn

C. Zhao
e-mail: zhaochunyan627@163.com

Introduction

Trunk sap flow velocity (V_S) is influenced by several variables including biological variables such as tree size, structure, and the leaf area index (LAI) (David et al. 2004; Kumagai et al. 2005; Si et al., 2007; Ewers et al. 2008; Chang et al. 2014) as well as environmental variables such as solar radiation, the vapor pressure deficit (VPD), air temperature (T_a), relative humidity (RH), and soil moisture (Pataki et al. 1998; O'Grady et al. 1999; Tang et al. 2006; Hernández-Santana et al. 2008; Tognetti., 2009). These biophysical variables affect V_S on multiple temporal and spatial scales. However, daily increases or decreases in

Published online: 13 September 2016

these environmental variables often do not produce the same V_S results. For example, under nominal VPD and soil moisture values, plants transpiration (or V_S) was higher in the morning than in the afternoon and evening hours. It therefore stands to reason that a hysteretic "loop" could indicate a decoupling of physiological processes from their environmental drivers. Clear evidence of hysteresis between V_S and canopy transpiration, which lasted from a few minutes to several hours, have been reported (Loustau et al. 1996; Staudt et al. 2011). We thus hypothesized that the hysteretic response pattern would also complicate understanding sap flow in relation to canopy microclimate.

Hysteresis is an important phenomenon affecting hourly patterns of transpiration. It also plays a significant ecological role in indentifying transpiration process and subsequently water cycling in natural forest systems, especially in arid environments, characterized by water scarcity and extreme climate conditions. Hysteretic response between V_S and environmental variables has been known for some time, but it has only gained attention in recent years (Zeppel et al. 2004; O'Grady et al. 2008; Matheny et al. 2014). V_S was either synchronous or lagged behind solar radiation or photosynthetically active radiation (PAR) and occurred in advance of VPD in humid environment (O'Brien et al. 2004; Oguntunde et al. 2005; Ma et al. 2008), semi-humid and semi-arid environment (Sun et al. 2010), and arid environment (Zheng and Wang., 2014). O'Grady (1999) reported greater hysteretic responses between V_S and VPD during the dry season than the wet season in a temperate forest, and other studies indicated that the magnitude of hysteretic response was positively correlated to maximal VPD (Zeppel et al. 2004; O'Grady et al. 2008). Moreover, since hysteretic relationship between transpiration (or V_S) and VPD has recently been linked to hydraulic limitations (Novick et al. 2014), a greater hysteretic lag was expected to occur in desert plants because of their significant hydrodynamic limitation in stomatal conductance. However, few studies have focused on identifying or incorporating hysteresis between V_S and meteorological variables in extreme arid environments.

The hydraulic lag mentioned above, used to quantify changes in plants water status throughout the day and the degree of hydrodynamic stress incurred by the plants, was mainly driven by daily hydrodynamic cycles and water storage depletion within the plants (Matheny et al. 2014). These responses were associated to soil moisture, VPD, and plant physiology. Changes in leaf water potential would result in a stomatal sensitivity to VPD, leaf water potential, and soil moisture (Thomas and Eamus, 2002). Therefore, as a mechanism of increasing resistance in the soil-plant-atmosphere continuum pathway, stomatal conductance could significantly decrease to maintain leaf water potentials above a critical threshold (Brodribb and Holbrook et al. 2006). Moreover, given that soil-root conductance declined with decreasing soil moisture around root systems on a daily scale, the corresponding soil-to-canopy hydraulic resistance could also produce hysteretic responses. Zheng et al. (2014) reported that sap flow typically began approximately 1 h earlier in branches than in stems and the fact that nighttime sap flow variation proved the contribution of plants in storing water for morning transpiration. As a result, tree stem water capacity could thus be another possible contributor to hysteresis. Consequently, hysteresis can be seen as a self-protection mechanism of plants to avoid the overlapping of peak V_S or transpiration and peak meteorological variables, which prevents excessive extraction of water from stems (Chen et al. 2011).

Whether the occurrence of hysteresis between V_S and meteorological variables will affect modeling processes related to sap flow remains unknown. O'Brien et al. (2004) indicated that hysteresis was either eliminated or significantly reduced in half-hourly V_S prediction when it was combined with light and VPD in an evaporative demand index, while Wang et al. (2011) found that hysteresis calibration improved effect of RH but decreased effect of PAR and T_a on V_S. Thus it is necessary to explore the underlying structure of co-varying meteorological data in evaluating the hysteretic response of V_S for all parts of a tree.

The Heihe River Basin (HRB) is one of the three largest inland river basins in the Hexi Corridor region of northwestern China. *Populus euphratica*, one of the structural species of the desert riparian forests located in the lower reaches of HRB, acts as natural barrier in maintaining the preservation of Ejina Oasis (Hou et al. 2010). Previous studies have led to considerable effort being focused on spatial patterns of sap flow along radial depths (Si et al. 2007), seasonal variation in evapotranspiration (ET) and its response to environmental factors (Hou et al. 2010), and hydraulic redistribution and hydraulic lift characteristics (Hao et al. 2010; Yu et al. 2013). However, to our knowledge, few studies have focused on hysteretic response of V_S to meteorological variables during growing season. In this study, *P. euphratica* V_S and associated environmental variables were monitored continuously during June–September 2012. The aim of this article is therefore to understand pattern and mechanism of hysteresis response between V_S and meteorological variables. The specific objectives of this study are as follows: (1) to quantify occurrence of hysteresis under different weather conditions, (2) to explore biophysical causes of hysteresis under an extreme arid environment, and (3) to understand hysteretic responses to V_S.

Materials and methods

Site description

This study was conducted at the Alxa Desert Eco-hydrology Experimental Research Station (42° 1′ 53.660″ N, 101° 3′ 13.265″ E, 884 m asl) in the lower HRB, northwest China. The climate in the region is characteristic of a continental arid zone, with an average precipitation of only 37.4 mm and annual pan evaporation in excess of 3390 mm. The average annual temperature is 8.2 °C. Prevailing wind directions are northwest in winter and spring and southwest to south in summer and autumn. Average annual wind speed is approximately 3.4 to 4.0 m/s. Soils are derived from fluvial sediments mixed with gray-brown desert deposits.

The experimental field used in the study was located at approximately 200 m southwest from the Alxa Desert Eco-hydrology Experimental Research Station and was protected by 100 m × 100 m fenced enclosures. A detailed plot inventory was conducted in July 2011. Dominant overstory vegetation consisted of *P. euphratica*, with 146 trees per ha^{-1} and a canopy cover of about 42 %. The next dominant species was *Tamarix ramosissima* with approximately 42 stems per ha^{-1}. The understory was dominated by grasses, including *Sophora alopecutoides*, *Achnatherum splendens*, and *Karelinia caspica*. Groundwater depth ranged from 1.93 to 2.65 m during the experimental period. Apart from precipitation, groundwater from the Heihe River provided the main sources of water to sustain regional ecosystems. Average age of *P. euphratica* specimens was 120 years old, average tree height (H, m) was 11.2 ± 2.4 m, and tree canopy dimensions ranged in an east to west direction from 2.5 to 11.3 m and in a south to north direction from 2.1 to 10.3 m. Average diameter at breast height (DBH) was 45.9 ± 14.4 cm and *P. euphratica* sapwood area (SA, cm^2) was determined by the drilling method. In total, 66 cores were extracted from a total of 66 trees, using an increment borer, from which the sapwood empirical formula was established. Average SA was approximately 305.74 ± 144.68 cm^2 (Table 1).

Sap flow velocity

We characterized tree model bin size by defining small, medium, and large trees as having DBH values <30, 30~65, and >65 cm, and both the DBH and the corresponding SA was at a maximal range of 30~65 cm range, of which the percentage was greater than 75 %. Thus three representative *P. euphratica* trees were randomly selected in a 10 m × 10 m subfence enclosure in the experimental field. Basic parameters were provided in Table 1. To monitor V_S during growing season of 2012 (June–September, days 168–276), we used heat ratio method (HRM) to determine continuous V_S in stems of the selected individuals. HRM probes (HRM30 ICT International Pty Ltd., Armidale, NSW, Australia) measured the ratio of the increases in temperature, following the release of a pulse of heat, at points equidistant downstream and upstream from the liner heater. A pair of copper-constantan thermocouples was symmetrically installed into the xylem tissue of the stems (north facing, 1.3 m height) 6 mm above and 6 mm below the center heater probe. Considering the radial distribution patterns of the sapwood, each thermocouple had two junctions to measure V_S, which were measured in the xylem tissues at 7.5 and 22.5 mm depth from the tip of the needle. A metal guide was used to aid in drilling holes and minimize probe misalignment during insertion. Pulses were sent every 30 min, and temperature ratios were recorded continuously by a data logger (SL5 Smart Logger, ICT, Australia). We calculated the heat pulse velocity (V_h, cm h^{-1}) according to the method of Burgess et al. (2001). All wound and misalignment corrections of probes were conducted according to Burgess et al. (2001). Since the xylem could not be cut to establish zero flow, we selected a series of overcast days at daybreak after a rainfall event where VPD was close to zero to establish the baseline. The final sap flow velocity (V_S) was then calculated according to the method of Burgess et al. (2001).

Meteorological variables

Meteorological variables, including PAR (mmol m^{-2} s^{-1}), temperature (T_a, °C), relative humidity (RH, %), and rainfall (mm), were recorded by a data logger as mean values of 30-min intervals. PAR was measured using a pyranometer (CM5, Kipp & Zonen, the Netherlands), and

Table 1 Biometric parameters of experimental *P. euphratica* trees used for sap flow measurements

	Tree age (year)	DBH (cm)	Height (m)	Canopy width (m)		SA (cm^2)
				East-West	South-North	
Quadrat	120	45.9 ± 14.4	11.2 ± 2.4	5.9 ± 1.6	5.9 ± 1.7	305.74 ± 144.68
Tree 1	102	43.4	12.9	5.3	7.8	274.97
Tree 2	127	52.3	12.6	8.2	8.6	358.72
Tree 3	118	47.3	16.3	6.4	8.8	327.39

Mean values of the quadart were calculated from 146 trees, and tree 1, tree 2, and tree 3 were selected as samples to monitor sap flow (mean ± SD)

DBH diameter at breast height, *SA* sapwood area

T_a and RH were measured using a Rotronic Sensor (RS2, Rotronic, Switzerland). Additionally, VPD was determined by T_a and RH according to the method of Campbell and Norman (1998):

$$\mathrm{VPD} = (1-\mathrm{RH}/100) \times 0.6108 \times e^{\left(\frac{17.27\times T_a}{T_a+237.3}\right)} \quad (1)$$

Leaf water potential and xylem hydraulic conductance

P. euphratica leaf water potential at pre-dawn (ψ_{pd}) and midday (ψ_m) was measured at, respectively, 5:30–6:00 h and 12:30–13:00 h using a Dewpoint Potentiometer (WP4, Decagon Devices, USA) every 5 days during measurements. All leaves were separately collected from the up-, middle- and down-canopy from a northern aspect to eliminate the influence of light. Leaves were immediately bagged and placed in a dark insulated container to prevent transpiration prior to measurement.

An established method derived from Darcy's law was used to calculate xylem hydraulic conductance proposed by Wullschleger et al. (1998):

$$K_p = \frac{E_{\max}}{\psi_{pd}-\psi_m} \quad (2)$$

where $E_{\max}$ is the maximum daily transpiration rate ($g\ m^{-2}\ s^{-1}$), which is usually closely aligned to the timing of midday water potential measurements (12:00–13:00 h) and is converted by midday V_S using SA; K_p is xylem hydraulic conductance ($g\ m^{-2}\ s^{-1}\ MPa^{-1}$); and ψ_{pd} and ψ_m are pre-dawn and midday leaf water potential (MPa), respectively.

Sap flow velocity hysteresis

Hysteretic effect occurred when an increase in a given independent variable does not cause the same variation in a dependent variable. We used cross-correlation coefficient plots between independent and dependent variables to identify their relationships at different time. Specifically, serial coefficients were respectively calculated between 30-min mean V_S observed at time *t* and corresponding meteorological variables (both forward and backward time *t*) at 30-min time step (for a total of 17 scenarios). When correlation coefficient between V_S and each environmental variable reached optimum, time lags were then regarded as actual hysteresis. Each meteorological variable was then partitioned into two separate groups, which included data during sunny days and data during cloudy and rainy days, as well as a third group that sunny day data further divided into larger values and smaller values. Subsequently, hysteretic patterns were quantified by plotting V_S as a function of each meteorological variable throughout daily flow according to the three groups. Shaped clockwise and anticlockwise loop characteristics were then used to identify hysteresis of the term.

Sap flow velocity model

Principal components analysis (PCA) has often been used to detect and interpret underlying structure of multiple co-varying variables. In this study, we used the PCA module in SPSS software (version 17.0) to analyze the underlying structure of 30-min meteorological data, which was the actual driver of V_S response for all parts of a tree collectively. Four general procedures were followed to construct a PCA-based sap flow velocity model relative to sunny days and rainy, cloudy days. First, a varimax rotation was applied to the PCA axis, and PCA factor scores were extracted from all original meteorological variables, including PAR, T_a, RH, and VPD, reducing the number of variables to model from four to a synthetic meteorological variable. Second, associated factor scores from observation of each 30-min interval of meteorological data from PCA were matched to simultaneous V_S observations. A three-parameter sigmoid function was then applied to predict *P. euphratica* V_S based on these factor scores. Finally, in order to emphasize V_S sensitivity to hysteresis, we developed another three-parameters sigmoid function to predict *P. euphratica* V_S based on new calibrated PCA factor scores, which were generated from the above mentioned synthetic meteorological variable after taking into account the specific hysteretic response. We named the latter method as "hysteresis calibration" in a subsequently study.

Canopy conductance

Although limited by leaf level stomatal conductance measurements, we predicted that canopy conductance (G_c, cm/s) would replace stomatal physiological processes. G_c was calculated following the method proposed by Monteith and Unsworth (1990):

$$G_{c=\frac{\lambda E\gamma}{36\rho c_p VPD}} \tag{3}$$

$$E = {}^{10\times\left(\overline{V_s}\sum_{i=1}^{n}\text{SA}\right)}\Big/_{A} \tag{4}$$

where λ is the latent heat of water vaporization (MJ kg^{-1}); E is hourly transpiration per ground area (mm h^{-1}); γ is the psychrometric constant (kPa °C^{-1}); ρ is air density (kg m^{-3}); c_p is the specific heat of air (MJ kg^{-1} °C^{-1}); $\bar{V}_s$ is the mean hourly sap flow velocity of the two representative trees; n is the number of trees in the experimental field; and A (cm^2) is the ground area of the enclosed fence plot.

Data analysis

Ten typical respective sunny days and ten typical respective cloudy and rainy days were selected to analyze diurnal patterns in V_S as well as the dominant associative meteorological variables, and specific time lags (min) and hysteretic magnitude were analyzed through cross-correlation and hysteretic loop size, for which one was for the upper curve and one was for the lower curve. Non-linear regression and partial correlation analysis were then used to examine canopy conductance control of V_S. Finally, V_S sensitivity to hysteresis was generated by a synthetic representation of an external meteorological variable, integrated through PCA-derived factors, including PAR, T_a, RH, and VPD. All statistical analyses were completed at the $P = 0.05$ level of confidence. These procedures were conducted with the Windows-based SPSS software version 17.0 (SPSS Inc., USA) and SigmaPlot software version 10.0 (Hearne Scientific Software Plc, Melbourne, Australia) (Fig. 1).

Results

Hysteresis between sap flow velocity and meteorological variables

Variation patterns in V_S were not consistent for PAR and VPD during typical sunny days, but they were approximately congruence to cloudy and rainy days (Fig. 2). However, pronounced hysteresis in V_S was observed as a function of meteorological variables under all weather conditions (Figs. 3 and 4). V_S occurred either earlier than VPD and RH by approximately 30 min or synchronous to T_a during the whole growing season, while V_S occurred after PAR approximately 60 to 90 min during both sunny and cloudy, rainy days. Plots between 30 min mean V_S, as opposed to meteorological variables, revealed a clockwise hysteresis for VPD and T_a but anticlo ckwise hysteresis for PAR and RH. During sunny days, the amount of clockwise hysteretic loop increased with increasing VPD and T_a regardless of soil moisture content, while conversely, the extent of anticlockwise hysteretic loop decreased with increasing PAR and RH under the same meteorological conditions. Both V_S and meteorological variables were significantly lower during cloudy and rainy days than during sunny days ($P = 0.00$, $n = 95$, independent-sample t test); however, pronounced hysteretic loop was also observed for mismatched patterns of variation in V_S and meteorological variables between morning and afternoon.

Biophysical control of hysteresis

The pattern of variation in canopy conductance (G_c) closely matched the pattern of variation in VPD after

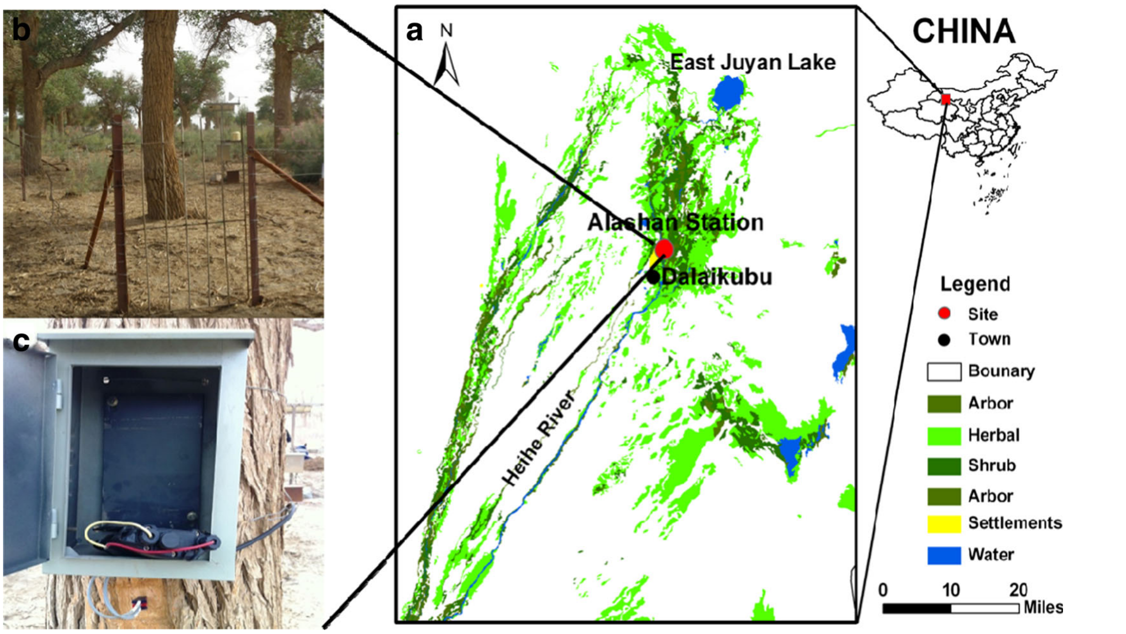

Fig. 1 **a** Location of study site in the lower reaches of Heihe River Basin, **b** spatial configuration of sampled *P. euphratica* trees in 10 m × 10 m fenced enclosures, and **c** measurement of sap flow velocity using the heat ratio method (HRM)

hysteretic calibration. For VPD under all meteorological conditions, exponential decay response was observed both during the morning and afternoon (with one exception in the afternoon as shown in Fig. 5c). Particularly for sunny days with higher VPD, the relationship between G_c and VPD indicated greater progressive stomatal closure in the afternoon than in the morning, following a gentle slope and a significant coefficient of determination. This indicated significantly sensitive in canopy conductance control in the morning, which caused the morning lag illustrated in Fig. 4. A negative partial correlation was observed between V_S and G_c (Table 2). Overall, with the exception of PAR on sunny days, partial correlation coefficients increased at different rates under hysteretic calibration. With increased partial correlation coefficients from 0.321 to 0.395 with synthetic VPD and PAR control variables, G_c was recognized as the principle biophysical index that impacted hysteresis. Moreover, the difference between ψ_{pd} and ψ_m ($\Delta\psi$), which were the driving force behind sap flow, declined as ψ_{pd} declined linearly under the $\Delta\psi = 0.26\psi_{pd} + 1.61$ equation. Moreover, *P. euphratica* hydraulic conductance during the growing season was generally less than 0.3 and a positive correlation between K_p and ψ_{pd} was found (Fig. 6).

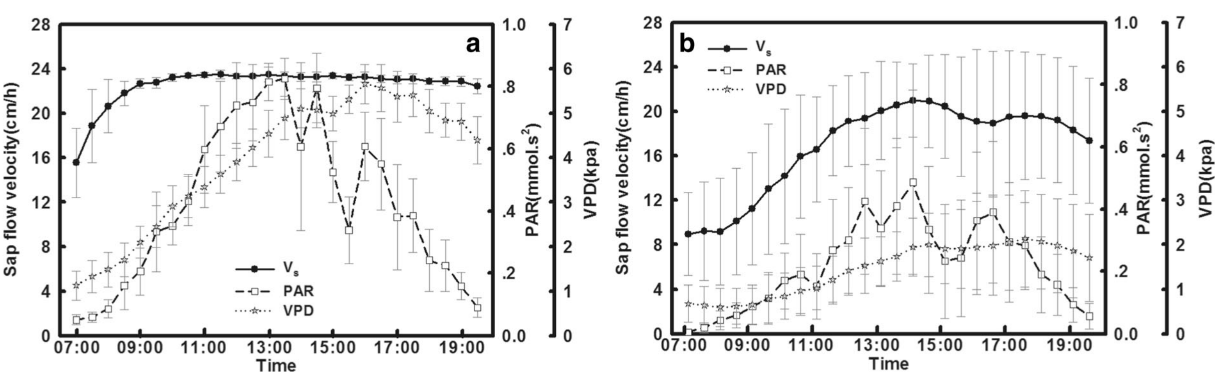

Fig. 2 Daily variations in mean sap flow velocity (V_S, *black solid line*), PAR (*short dashed line*) and VPD (*dotted line*), on **a** 10 sunny days and on **b** 10 days in cloudy and rainy days

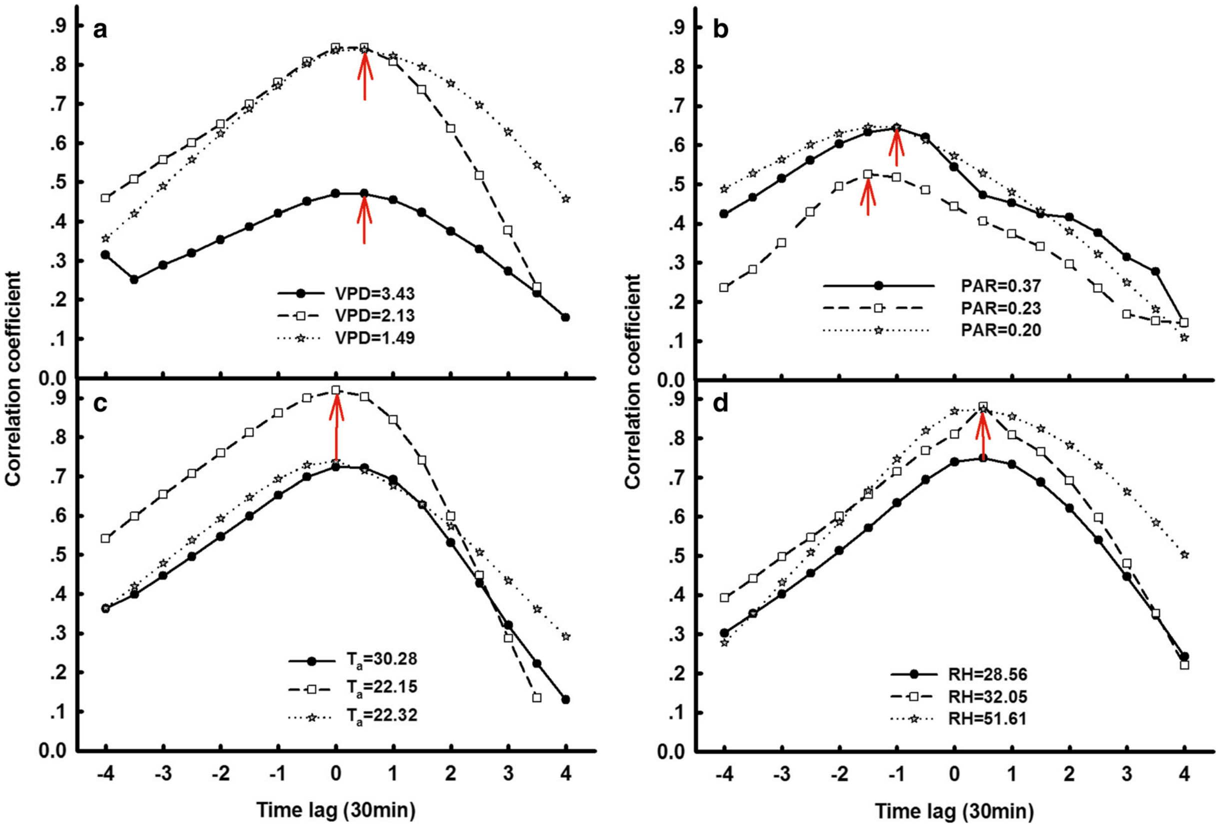

Fig. 3 Time lags of multiple meteorological variables on sap flow velocity. *Black circles* and *white squares* denote data on sunny days during respective June to August and September. *Gray stars* denote data on cloudy and rainy days during June to September, and *red arrows* denote the maximum correlation coefficient

Response of meteorological variables on sap flow velocity

PCA was conducted to quantify hysteretic response from synthetic meteorological variables on V_S (Table 3). Two PCA components accounted for 86.56 and 89.58 % of total variance in meteorological variables without taking into account hysteresis during sunny days and cloudy, rainy days, respectively, of which 85.25 and 88.88 % was explained by the hysteresis calibration model. Although the cumulative percentage did not show significant increase in both hysteresis calibration models, PC1 improved from 68.38 to 73.73 % on sunny days, as well as 68.76 to 75.56 % on cloudy and rainy days when hysteresis was taken into account. Based on the principal component eigenvalues, the synthetic meteorological index integrated from the weighted average of PC1 and PC2 was calculated. A strong Sigmoid ("S") curve was matched between V_S and the synthetic meteorological factors both for non-hysteresis and hysteresis calibration models (Fig. 7). However, compared to the non-hysteresis model, especially on sunny days, scatter diagram points were more tightly bound and correlated under the hysteresis model. Moreover, the coefficient of determination of the regression model increased by approximately 56 % (from 0.50 to 0.78) and 36 % (from 0.45 to 0.61) after hysteresis was calibrated to sunny days and cloudy, rainy days.

Discussions

Hysteresis in *P. euphratica* sap flow-meteorological relationships in an arid region

Understanding time lag or hysteresis between V_S and meteorological variables allows researchers to identify relationships between trunk V_S and the sum total of tree transpiration (Lu et al. 2004). Although V_S and meteorological variables were significantly higher on sunny

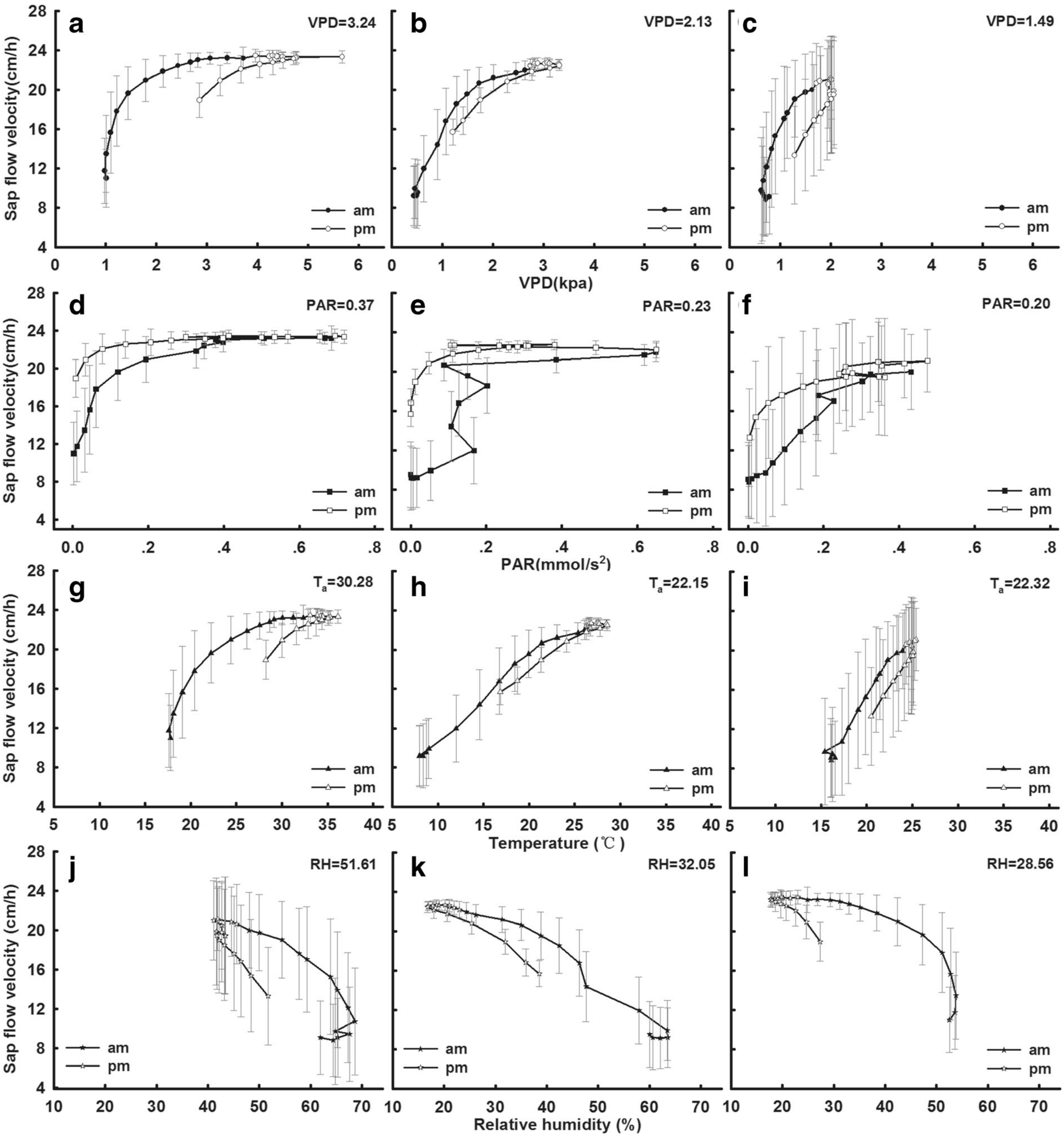

Fig. 4 Hysteretic response of 30 min mean sap flow velocity to VPD (**a**–**c**), PAR (**d**–**f**), T_a (**g**–**i**), and RH (**j**–**l**). *Filled in symbols* denote values in the morning, and *non-filled in symbols* denote values in the afternoon; the magnitude of hysteresis loops on sunny days is shown on the *left* and in the *middle*, while the magnitude of hysteresis loops on cloudy and rainy days is shown on the *right*

days compared to cloudy and rainy days, pronounced asynchronous patterns were observed on both sunny and cloudy, rainy days, but no deviation was found between V_S and T_a. This occurred when PAR was in advance of VPD and RH lagged behind of V_S. Moreover, no seasonal variation in hysteresis was observed under different VPD and RH (Figs. 2 and 3). Parallel results were compared to other studies under different meteorological conditions. For example, Wang et al. (2009) reported that V_S came in advance of VPD by

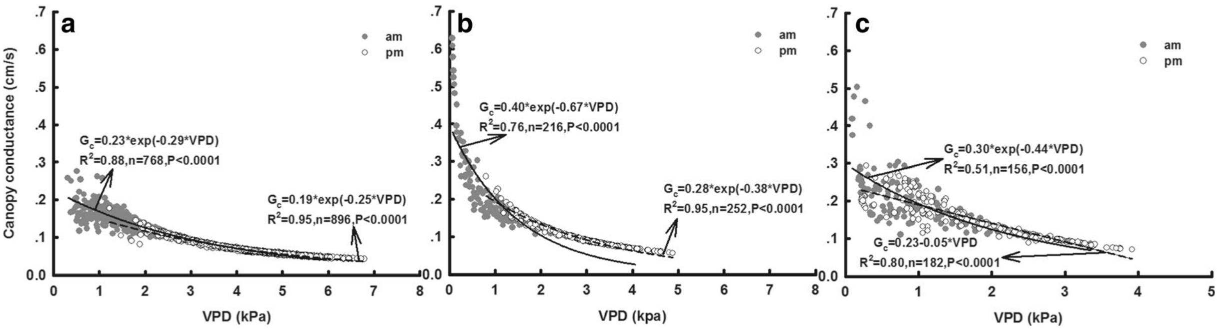

Fig. 5 Relationships between canopy conductance after hysteretic calibration and VPD in the morning (*gray circles*) and in the afternoon (*white circles*); **a** averaged VPD is 3.43 kPa; **b** averaged VPD is 2.13 kPa; and **c** averaged VPD is 1.49 kPa

approximately 47 to 130 min but lagged behind total radiation by approximately 10 to 70 min for seven common tree species found in the Beijing areas. Similarly, data also concluded that PAR came in advance of V_S by approximately 10 min and approximately 10 to 40 min for *poplar* in semi-humid and semi-arid environments, respectively (Sun et al. 2010), while there was an approximate 50 to 120 and 110 min lag after VPD and RH for *poplar* and *Cassava*, respectively, under humid environmental conditions (Oguntunde et al. 2005). On the other hand, no obvious hysteresis associated with *RH* was found during the summer and autumn for *Larix gmelinii* in a semi-humid environment (Wang et al. 2011). Contrary to the results above, however, significant and complex hysteresis was observed in V_S to PAR and slight hysteresis in V_S to VPD for *P. euphratica* investigated in this study, which could be attributed to specific species drought tolerance, such as conditions under relative low water availability and those that were under predominant control from VPD but not PAR. Hysteresis also showed a seasonal trend for *Acacia mangium* and *poplar* (Ma et al. 2008; Sun et al. 2010), which is different from the results found in this study. The difference might arise because the PAR and VPD gradient during our study period was much narrower than those in humid and semi-arid locality (Li et al. 2016), where plants mainly relied on rainfall and shallow soil moisture during growing season.

Table 2 Partial correlation coefficients (*R*) between V_S and canopy conductance

Control variable		Non-hysteresis	Hysteresis calibration
V_S		Canopy conductance	
R	VPD	−0.366**	−0.471**
R	PAR (sunny)	−0.886**	−0.880**
R	PAR (cloudy)	−0.656*	−0.720**
R	VPD and PAR	−0.321**	−0.395**

*Correlations are significant at $P < 0.05$; **Correlations are significant at $P < 0.01$

Biophysical control on hysteresis

During the morning, as VPD and T_a increased, V_S also increased. In the afternoon, however, V_S at any nominal VPD or T_a was lower compared to the morning. A clockwise rotation response curve was evident, which resulted from an increase in atmospheric evaporative demands (Fig. 4a–c, g–i). O'Brien et al. (2004) observed a similar hysteresis in V_S response to VPD for *Callitris glaucophylla* and *Eucalyptus crebra* during prolonged and extensive droughts and attributed this afternoon hysteretic effect that resulted in stomatal closure either a response to higher VPD, decreasing light (PAR) levels, or internal cycling. A low decoupling coefficient less than 0.2 indicated that *P. euphratica* was well coupled with the atmosphere and able to exert effective stomatal control over V_S or transpiration in response to environmental stresses (Li et al. 2013). Compared to the non-hysteresis model, patterns of variation and peaks in V_S to some extent were synchronized to G_c, VPD, and RH after hysteretic calibration. Moreover, the strong exponential decay response of G_c to VPD in the afternoon (Fig. 5) indicated progressively increasing stomatal closure in the canopy as a response to increasing VPD, which reduced overall tree water use. At the same time, a 29 % improvement in partial correlation coefficients from 0.366 to 0.471, which derived from hysteretic calibration of VPD, further verified the physiological control of hysteresis (Table 2). This conclusion was consistent studies on native tree species in a temperate region in Australia (Zeppel et al. 2004), urban tree

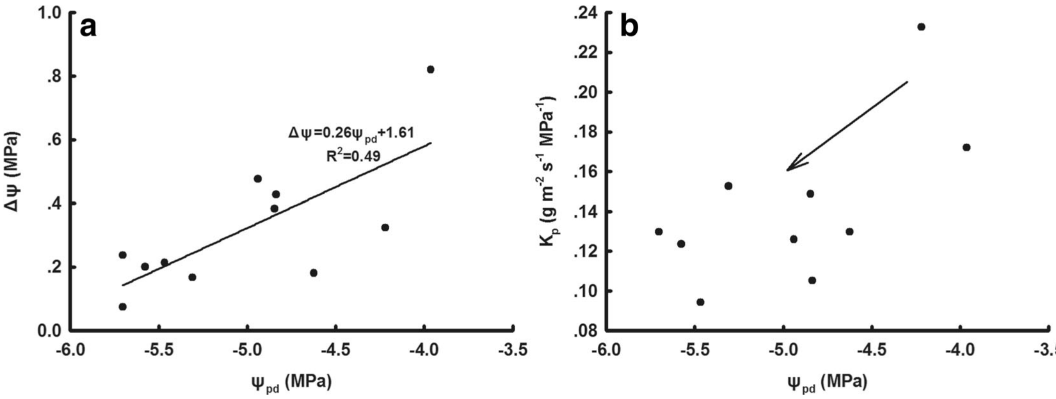

Fig. 6 **a** Relationships between pre-dawn leaf water potential (ψ_{pd}) and the difference ($\Delta\psi$) between ψ_{pd} and midday leaf water potential during June to September. **b** Relationships between xylem hydraulic conductance, estimated as the slope of sap flow, and pre-dawn leaf water potential

species in North China (Chen et al. 2011), and desert plants in the Gurbantünggüt Desert, northwest China (Zheng and Wang., 2014). Moreover, the pattern and magnitude of hysteresis loops were also related to daily hydrodynamic cycling, which could be indicative of relative changes in plant water status throughout the day (Matheny et al. 2014). Lower leaf water potential in the afternoon compared to the morning caused decreased stomatal conductance and, subsequently time lags or hysteresis to occur (Eamus and Prior, 2001). However, different to American red maples, of which would regulate their stomatal conductance to keep leaf water potential relatively constant throughout the day (Thomsen et al. 2013), the response of *P. euphratica* was to decrease G_c to maintain their leaf water potentials above a critical threshold under imbalance between water demands related to the atmosphere and water supplies related to soil-to-canopy flow.

Alternatively, increases in soil-to-canopy resistance as soil-root conductance declined with decreasing soil moisture around root systems could explain hysteresis between V_S and VPD (Zeppel et al. 2004). Chen et al. (2011) reported that an increase in resistance increased in soil-plant-atmosphere continuum (SPAC) pathway on

Table 3 Eigenvalue, percentage, cumulative percentage, and principal component loadings of principal components analysis (PCA)

		Eigenvalue		Percentage		Cumulative percentage	
Sunny		PC1	PC2	PC1	PC2	PC1	PC2
	A	2.74	0.73	68.38	18.18	68.38	86.56
	B	2.95	0.46	73.73	11.52	73.73	85.25
Cloudy	A	2.75	0.83	68.76	20.82	68.76	89.58
	B	3.02	0.53	75.56	13.32	75.56	88.88
			Factor loadings				
				PAR	VPD	T_a	RH
Sunny	A		PC1	0.38	0.52	−0.53	−0.53
			PC2	0.92	−0.35	0.15	0.15
	B		PC1	0.49	0.48	−0.51	−0.51
			PC2	−0.54	0.79	0.28	0.28
Cloudy	A		PC1	0.32	0.59	−0.51	−0.51
			PC2	0.90	−0.21	0.37	0.37
	B		PC1	0.44	0.56	−0.49	−0.49
			PC2	0.85	−0.24	0.47	0.47

A without hysteresis, *B* with hysteresis

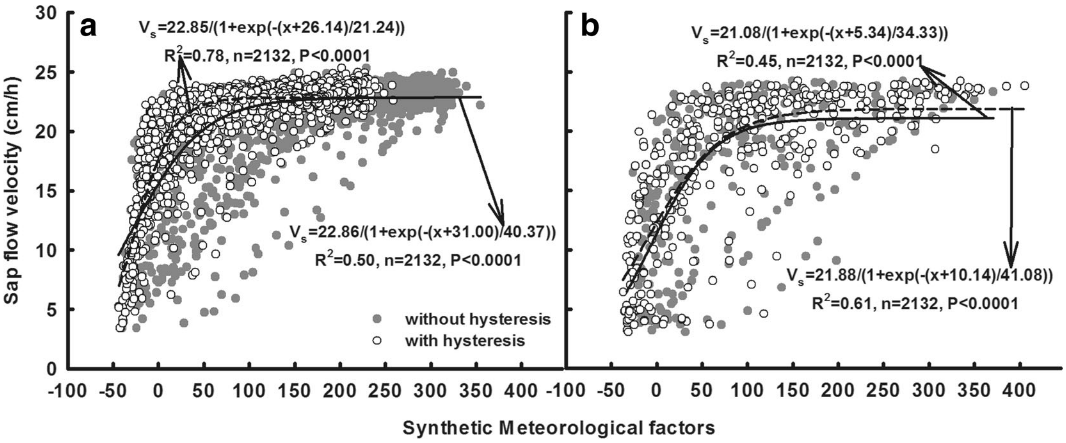

Fig. 7 Regression analysis between synthetic meteorological variables and sap flow **a** on sunny days with hysteresis (*white circles*) and without hysteresis (*gray circles*) as well as **b** on cloudy and rainy days with hysteresis (*white circles*) and without hysteresis (*gray circles*); *straight lines* and *dotted lines* denote the non-hysteresis model and the hysteresis calibrated model, respectively

a diurnal basis would induce hysteresis at a higher daily average VPD. However, O'Grady et al. (2008) emphasized that the size of hysteresis was largely the result of VPD instead of decreasing soil-to-leaf conductance because hysteresis, in the relationship between transpiration and VPD, was observed in both irrigated and rainfed *Eucalyptus globulus* trees. Main water sources of *P. euphratica* changed from available water in a single soil layer to deep available subsoil water and groundwater as groundwater depth increased from 1.80 to 3.25 m (Si et al. 2014). Thus, the decreasing of groundwater table (from 1.93 to 2.65 m) during the research period might have slightly increased resistance in soil-to-canopy water transport, which may explain the hysteresis effect following progressive drought stress. David et al. (2007) attributed difference between ψ_{pd} and ψ_m, which was previously attributed to hydrodynamic water potential gradients from roots to shoots, as the driving force of midday sap flow. Moreover, the declining trend in $\Delta\psi$ following declining ψ_{pd} (Fig. 6a) indicated a relatively lower sap flow driving force under progressive drought, which provides evidence of the existence of critical leaf water potential. Therefore, isohydric control of plant water status through stomatal downregulation of transpiration (or V_S) benefitted in preventing water potential falling to a critical threshold and thereby maintaining xylem functions (Franks et al. 2007; O'Grady et al. 2008), which was in agreement to the above analysis. Surprisingly, when compared to sunny days, the threshold of G_c was larger than observed on cloudy and rainy days, while the absolute threshold of hysteresis was exhibited on cloudy and raining days when V_S and VPD were relatively lower. This could be related to the sensitivity of desert species to VPD, leaf water potential, and wetter conditions.

Compared to other riparian tree species, such as *E. globulus*, *Melaleuca argentea*, and *Corymbia bella* in northern Australia (O'Grady et al. 2006, 2008), relatively lower K_p values were found for *P. euphratica* in this study. Lower hydraulic conductance for trees was assumed to be a feature of drought tolerance, which has a tendency to limit sap flow from roots to leaves and promotes higher conservation of water use (Lemoine et al. 2001; David et al. 2007). Martinez-Vilalta et al. (2002) reported on a trade-off between hydraulic efficiency and resistance to xylem cavitation. The positive relationship between K_p and ψ_{pd} (Fig. 6b) provided evidence for increasing resistance along root-to-leaf hydrodynamics and thereby *P. euphratica* hysteresis. This, however, requires further study.

Furthermore, Zheng et al. (2014) attributed the hysteretic nature of transpiration to the depletion of internal plant water throughout the day and the time lag between VPD and PAR. Chuang et al. (2006) indicated that plant water storage capacity was behind the postponement of V_S response to driving variables and the adjustment for the time lag between V_S and transpiration. Additionally, Zheng and Wang (2014) stood in support of the contribution of stored water to the promotion of hysteresis through confirmed nighttime sap flow of desert *Haloxylon ammodendron*. Nighttime V_S for *P. euphratica* stands was observed throughout the night and accounted for 31–47 % of its daily V_S during 2012 growing season (Si et al. 2015). Thus, we proposed that the contribution of stored water in trunks to transpiration (or V_S) could also contribute to hysteretic response.

In contrast to the clockwise hysteretic pattern observed in response to VPD and T_a on V_S in the morning, at a given value of PAR, VPD was lower than that observed in the afternoon and V_S was higher in the afternoon than in the morning (Fig. 2). Thus, an alternative anticlockwise response of PAR on V_S was observed (Fig. 4d–f). Morning lag in V_S in response to PAR could be explained by water capacitance in the stems, a slow stomatal response to PAR, boundary layer dynamics, or by the limitation of diffusion by wet leaves (O'Brien et al. 2004). Moreover, Zeppel et al. (2004) attributed the phenomenon to the fact that even through peak levels of solar radiation occur at the solar noon, VPD peaks in the mid-afternoon and stomatal conductance became light saturated at low levels of light. For *P. euphratica*, this study found that a 9 % increasing in partial correlation coefficients on cloudy and rainy days after hysteretic calibration (Table 3) translated into a slow stomatal response to PAR, which effectively verified canopy stomatal biophysical control of morning lag.

Feedback of hysteresis between sap flow and synthetic meteorological variables to water use

Synthetic meteorological variables, retaining most information but eliminating intersections and covariance found in the original variables through PCA, were used to analyze the hysteretic feedback response of V_S. Similar to *poplar* species in northeastern China (Sun et al. 2010), a strong sigmoid curve was fitted between V_S and synthetic meteorological variables for both non-hysteresis and hysteresis calibration models. This could be attributed to the lower representation of total variance and coefficient of determination of sigmoid curves (Table 3; Fig. 7) regardless of water scarcity during the growing season. O'Brien et al. (2004) indicated that time lags and hysteresis between V_S and meteorological variables would be less important when averaged over a day by PCA. In contrast, hysteresis in the present study was still distinct as the tightly bound scatter diagram and the significant improvement in coefficient of determination (0.50 to 0.78) showed through hysteretic calibration on sunny days. However, the slightly improvement observed in sigmoid function on cloudy and rainy days could be an indicator of the lack of importance of hysteretic calibration under this particularly meteorological condition.

Conclusions

VPD, T_a, RH, and PAR impact *P. euphratica* V_S, but more importantly, we showed that the response of V_S to each environmental variable was different in the morning compared to the afternoon. Difference patterns between V_S and environmental variables within a period of a day could be attributable to differences in canopy conductance regulation of V_S or transpiration. A strong sigmoid function could be used to predict V_S during the growing season form synthetic meteorological variables when taking hysteresis into account. These findings will aid in the comprehensive understanding of mechanisms related to hourly patterns of V_S or transpiration of *P. euphratica*, as well as for catchment hydrology in desert riparian stands in extreme arid regions. Furthermore, future research should also consider interactive impacts of biological morphology and trunk water storage forces on *P. euphratica*.

Acknowledgments This study was supported by the National Natural Science Foundation of China (91225301, 912253003), the Key Project of the Chinese Academy of Sciences (KZZD-EW-04-05), and the West Light Foundation of Chinese Academy of Sciences.

Reference

Brodribb, T. J., & Holbrook, N. M. (2006). Declining hydraulic efficiency as transpiring leaves desiccate: two types of response. *Plant Cell and Environment, 29*, 2205–2215.

Burgess, S. S. O., Adams, M. A., Turner, N. C., Beverly, C. R., Ong, C. K., Khan, A. A. H., & Bleby, T. M. (2001). An improved heat pulse method to measure low and reverse rates. *Tree Pyhsiology, 21*(9), 589–598.

Campbell, G. S., & Norman, J. M. (1998). An introduction to environment biophysics. *Springer Netherlands Publisher*, 37–75.

Chang, X. X., Zhao, W. Z., & He, Z. B. (2014). Radial pattern of sap flow and response to microclimate and soil in Qinghai spruce (*Picea crassifolia*) in the upper Heihe River Basin of arid northwestern China. *Agricultural and Forest Meteorology, 187*, 14–21.

Chen, L. X., Zhang, Z. Q., Li, Z. D., Tang, J. W., Caldwell, P., & Zhang, W. J. (2011). Biophysical control of whole tree transpiration under an urban environment in Northern China. *Journal of Hydrology, 402*, 388–400.

Chuang, Y. L., Oren, R., Bertozzi, A. L., Phillips, N., & Katul, G. G. (2006). The porous media model for the hydraulic system of a conifer tree: linking sap flux data to transpiration rate. *Ecological Modelling, 191*, 447–468.

David, T. S., Ferrcira, M. I., Cohen, S., Pereira, J. S., & David, J. S. (2004). Constraints on transpiration from an evergreen oak tree in southern Portugal. *Agricultural and Forest Meteorology, 122*, 193–205.

David, T. S., Henriques, M. O., Kurz-Besson, C., Nunes, J., Valente, F., Vaz, M., Pereira, J. S., Siegwolf, R., Chaves, M. M., Gazarini, L. C., & David, J. S. (2007). Water-use strategies in two co-occurring Mediterranean evergreen oaks: surviving the summer drought. *Tree Physiology, 27*, 793–803.

Eamus, D., & Prior, L. (2001). Ecophysiology of trees of seasonally dry tropics: comparison among phonologies. *Advanced in Ecological Research, 32*, 113–198.

Ewers, B. E., Mackay, D. S., Tang, J., Bolstad, P. V., & Samanta, S. (2008). Intercomparison of sugar maple (*Acer saccharum* Marsh.) stand transpiration responses to environmental conditions from the Western Great Lakes Region of the United States. *Agricultural and Forest Meteorology, 148*, 231–246.

Franks, P. J., Drake, P. L., & Froend, R. H. (2007). Anisohydric but isohydrodynamic: seasonally constant plant water potential gradient explained by a stomatal control mechanism incorporating variable plant hydraulic conductance. *Plant, Cell and Environment, 30*, 19–30.

Hao, X. M., Chen, Y. N., Li, W. H., Guo, B., & Zhao, R. F. (2010). Hydraulic lift in *Populus euphratica Oliv* from the desert riparian vegetation of the Tarim River Basin. *Journal of Arid Environments, 74*, 905–911.

Hernández-Santana, V., Dacid, T. S., & Martínez-Fernández (2008). Environmental and plant-based controls of water use in a Mediterranean oak stand. *Forest and Ecology Management, 255*, 3707–3715.

Hou, L. G., Xiao, H. L., Si, J. H., Xiao, S. C., Zhou, M. X., & Yang, Y. G. (2010). Evapotranspiration and crop efficient of *Populus euphratica Oliv* forest during the growing season in the extreme arid region northwest China. *Agricultural Water Management, 97*, 351–356.

Kumagai, T., Aoki, S., Nagasawa, H., Mabuchi, T., Kubota, K., Inoue, S., Utsumi, Y., & Otsuki, K. (2005). Effect of tree-to-tree and radial variations on sap flow estimates of transpiration in Japanese cedar. *Agricultural and Forest Meteorology, 135*, 110–116.

Lemoine, D., Peltier, J. P., & Marigo, G. (2001). Comparative studies of the water relations and the hydraulic characteristics in *Fraxinus excelsior*, *Acer pseudoplatanus* and *A. opalus* trees under soil water contrasted conditions. *Annals of Forest Science, 58*, 723–731.

Li, W., Si, J. H., Feng, Q., & Yu, T. F. (2013). Response of transpiration to water vapor pressure of *Populus euphratica*. *Journal of Desert Research, 33*(5), 1–8 (in Chinese).

Li, W., Si, J. H., Yu, T. F., & Li, X. Y. (2016). Response of Populus euphratica Oliv. sap flow to environmental variables for a desert riparian forest in the Heihe River Basin, Northwest China. *Journal of Arid Land, 8*(4), 1–13.

Loustau, D., Berbigier, P., Roumagnae, P., Arruda-PCAheo, C., David, J. S., Ferreira, M. I., Pereira, J. S., & Tavares, R. (1996). Transpiration of a 64-year-old maritime pine stand in Portugal. 1. Seasonal course of water flux through maritime pine. *Oecologia, 107*, 33–42.

Lu, P., Brban, L., & Zhao, P. (2004). Granier's thermal dissipation probe (TDP) method for measuring sap flow in trees: theory and practice. *Acta Botanica Sinica, 46*(6), 631–646.

Ma, L., Lu, P., Zhao, P., Rao, X. Q., Cai, X. A., & Zeng, X. P. (2008). Diurnal, daily, seasonal, and annual patterns of sap-flux-scaled transpiration from an *Acacia mangium* plantation in South China. *Annals of Forest Science, 65*(4), 1–9.

Martínez-Vilalta, J., Prat, E., Oliveras, I., & Piñol, J. (2002). Xylem hydraulic properties of roots and stems of nine Mediterranean woody species. *Oecologia, 133*, 19–29.

Matheny, A. M., Bohrer, G., Vogel, S. S., Morin, T. H., He, L. L., Frasson., R. P. D. M., Mirfenderesgi, G., Schāfer, K. V. R., Gough, C. M., Ivanov, V. Y., & Curtis, P. S. (2014). Species-specific transpiration responses to intermediate disturbance in a northern hardwood forest. *Journal of Geophysical Research: Biogeoscience, 119*, 2292–2311.

Monteith, J. L., & Unsworth, M. H. (1990). Principals of environmental physics. 2nd edition. Edward Arnold, London.

Novick, K. S., Brantley, C. F., Miniat, J. W., & Vose, J. M. (2014). Inferring the contribution of advection to total ecosystem scalar fluxes over a tall forest in complex terrain. *Agricultural and Forest Meteorology, 185*, 1–13.

O'Brien, J. J., Oberbauer, S. F., & Clark, D. B. (2004). Whole tree xylem sap flow responses to multiple environmental variables in a wet tropical forest. *Plant, Cell and Environment, 27*, 551–567.

O'Grady, A. P., Eamus, D., & Hutley, L. B. (1999). Transpiration increases during the dry season: pattern of tree water use in eucalypt open-forests of northern Australia. *Tree Physiology, 19*, 591–597.

O'Grady, A. P., Eamus, D., Cook, P. G., & Lamontagne, S. (2006). Comparative water use by the riparian *Melaleuca argentea* and *Corymbia bella* trees in the wet-dry tropics of northern Australia. *Tree Physiology, 26*, 219–228.

O'Grady, A. P., Worledge, D., & Battaglia, M. (2008). Constraints on transpiration of *Eucalyptus globulus* in southeastern Tasmania, Australia. *Agricultural and Forest Meteorology, 148*, 453–465.

Oguntude, P. G. (2005). Whole-plant water use and canopy conductance of cassava under limited available soil water and varying evaporation demand. *Plant and Soil, 278*, 371–383.

Pataki, D. E., Oren, R., Katul, G., & Sigmon, J. (1998). Canopy conductance of *Pinus taeda*, *Liquidambar styraciflua* and *Quercus phellos* under varying atmospheric and soil water conditions. *Tree Physiology, 18*, 307–315.

Si, J. H., Feng, Q., Zhang, X. Y., Chang, Z. Q., Su, Y. H., & Xi, H. Y. (2007). Sap flow of *Populus euphratica* in a desert riparian forest in an extreme arid region during the growing season. *Journal of Integrative Plant Biology, 49*(4), 425–436.

Si, J. H., Feng, Q., Cao, S. K., Yu, T. F., & Zhao, C. Y. (2014). Water use sources of desert riparian *Populus euphratica* forests. *Environmental Monitoring and Assessment., 186*(9), 5469–5477.

Si, J. H., Feng, Q., Yu, T. F., & Zhao, C. Y. (2015). Nighttime sap flow and its driving forces for *Populus euphratica* in a desert riparian forest, Northwest China. *Journal of Arid Land, 7*(5), 665–674.

Staudt, K., Serafimovich, A., Siebicke, L., Pyles, R. D., & Falge, E. (2011). Vertical structure of evapotranspiration at a forest site (a case study). *Agricultural and Forest Meteorology, 151*, 709–729.

Sun, D., Guan, X. D., Yuan, F. H., Wang, Z. A., & Wu, J. B. (2010). Time lag effect between poplar's sap flow velocity and microclimate factors in agroforestry system in West Liaoning Province. *Chinese Journal of Applied Ecology, 21*(11), 2742–2748 (in Chinese).

Tang, J., Bolstad, P., Ewers, B., Desai, A., Davis, K., & Carey, E. (2006). Sap flux-upscaled canopy transpiration, stomatal conductance, and water use efficiency in an old growth forest in the Great Lakes region of the United States. *Journal of Geophysical Research: Biogeosciences, 111*, –12.

Thomas, D. S., & Eamus, D. (2002). Seasonal patterns of xylem sap PH, xylem abscisic acid concentration, leaf water potential and stomatal conductance of six evergreen and deciduous Australian savanna tree species. *Australian Journal of Botany, 50*, 229–236.

Thomsen, J. E., Bohrer, G., Matheny, A. M., Ivanov, V. Y., He., L. L., Renninger, H. J., & Tchāfer, K. V. R. (2013). Contrasting hydraulic strategies during dry soil conditions in *Quercus rubra* and *Acer rubrum* in a sandy site in Michigan. *Forests, 4*, 1106–1120.

Tognetti, R., Giovannelli, A., Lavini, A., Morelli, G., Fragnito, F., & D'Andria, R. (2009). Assessing environmental controls over conductances through the soil-plant-atmosphere continuum in an experimental olive tree plantation of southern Italy. *Agricultural and Forest Meteorology, 149*, 1229–1243.

Wang, H., Ouyang, Z. Y., Zhang, H., Wang, X. K., Ni, Y. M., & Ren, Y. F. (2009). Time lag characteristics of stem sap flow of common tree species during their growing season in Beijing downtown. *Chinese Journal of Applied Ecology, 20*(9), 2111–2117 (in Chinese).

Wang, H. M., Sun, W., Zu, Y. G., & Wang, W. J. (2011). Complexity and its integrative effects of the time lags of environment factors affecting *Larix gmelinii* stem sap flow. *Chinese Journal of Applied Ecology, 22*(12), 3109–3116 (in Chinese).

Wullschleger, S. D., Meinzer, F. C., & Vertessy, R. A. (1998). A review of whole-plant water use studies in trees. *Tree Physiology, 18*, 499–512.

Yu, T. F., Feng, Q., Si, J. H., Xi, H. Y., Li, Z. X., & Chen, A. F. (2013). Hydraulic redistribution of soil water by roots of two desert riparian phreatophytes in northwest China's extremely arid region. *Plant and Soil, 372*, 297–308.

Zeppel, M. J. B., Murray, B. R., Barton, C., & Eamus, D. (2004). Seasonal responses of xylem of xylem sap velocity to VPD and solar radiation during drought in a stand of native trees in temperate Australia. *Functional Plant Biology, 31*, 461–470.

Zheng, C. L., & Wang, Q. (2014). Water-use response to climate factors at whole tree and branch scale for a dominant desert species in central Asia: *Haloxylon ammodendron*. *Ecohydrology, 7*, 56–63.

Zheng, H., Wang, Q., Zhu, X., Li, Y., & Yu, G. (2014). Hysteresis responses of evapotranspiration to meteorological factors at a Diel timescale: patterns and causes. *PloS One, 9*(6), e98857. doi:10.1371/journal.pone.0098857.